

Chapter 2

Targeting and Excitation of Photoactivatable Molecules: Design Considerations for Neurophysiology Experiments

Eugene F. Civillico, J. Peter Rickgauer, and Samuel S.-H. Wang

Abstract

Each chapter in this volume describes in detail the application of one or a group of photosensitive molecules to biological research. In this chapter, we take up general prefatory questions: how to determine which molecules are appropriate to use, and what type of compound delivery and light-targeting apparatus for photoactivation is likely to give satisfactory spatial and temporal performance. We enumerate the advantages and disadvantages of currently available “caged” and genetically encoded photosensitive molecules. We also compare current mature and emerging technologies for patterned light delivery, referring as much as possible to broadly applicable general principles. Our goal is to provide a comprehensive overview with signposts to more detailed treatments.

Key words: Caged compound, Channelrhodopsin, Scanning, AOD, Galvanometric, Holographic, Beamsteering

1. Families of Photoactivatable Molecules

Photoactivatable molecules are available that influence a wide range of extracellular and intracellular neurophysiological functions. The choice and availability of photosensitive molecule depend on the research question and will influence subsequent choices in the design of experimental apparatus. The first major choice is whether to use photolysis-activated “caged” diffusible molecules (Sect. 2.1) or light-sensitive membrane proteins (Sect. 2.2).

For activation of native receptors with a time course matching endogenously occurring binding, unbinding, and biochemical kinetics, caged compounds are preferred. In general, newer optogenetic approaches are attractive when “on–off” control of neuronal

membrane potential or intracellular cascades is desired as a means of determining the downstream effects on other cells. More importantly, optogenetic probes are proteins that can be expressed specifically in genetically identifiable cell types. Because by definition these approaches involve introducing and manipulating foreign molecular machinery, the effects on the manipulated cell or cells themselves have the potential to go outside the normal range of function. Topics in single-cell physiology such as dendritic integration are still best explored with caged compounds.

1.1. Caged Compounds

1.1.1. Caged Ionotropic Receptor Agonists and Antagonists

Ionotropic neurotransmitter mechanisms consist of initiation of one or more transmembrane currents. The first caged neurotransmitters were acetylcholine receptor agonists (1, 2, 45), followed by the first caged glutamate (3). Innovation in caged glutamates has resulted in improved usability for both conventional one-photon UV illumination and IR-based two-photon activation (see Sect. 4), leading to the development of the 6-bromo-7-hydroxycoumarin-4-ylmethyl (BHC) and 4-methoxy-7-nitroindolinyl (MNI) protecting groups (4–6). The most widely used caged glutamate is MNI-glutamate, which combines a high absorption coefficient and high quantum yield ($4,300 \text{ M}^{-1} \text{ cm}^{-1}$ and 0.085 at 350 nm, respectively; (7)), with relatively low toxicity and interference with signaling pathways.

Glutamate receptor subtype-specific ligands have also been caged, including NMDA (8), kainate (9), and D-aspartate (10, 11). Other promising improvements are 4-carboxymethoxy-5,7-dinitroindolinyl (CDNI) with increased absorption and quantum yield and reduced nonspecific effects (12) and RuBi-glutamate, which is based on novel ruthenium-based photochemistry and is photolyzed by visible light (13).

Other useful caged transmitters include caged GABA (14), which has seen recent innovations in the form of new caging groups to reduce pharmacological side effects and improve optical properties (15–17), and coumarin-caged glycine, which can be activated by visible light (18).

Although the transmembrane currents mediated by these receptors may potentially be mimicked using light-activated engineered channels, reproducing the kinetics of native receptors is a nontrivial task. When receptor populations at single synapses are heterogeneous, the native ligand may activate multiple receptor subtypes at once. For example, channelrhodopsin-mediated currents cannot currently emulate the coincidence detection properties of a synapse that includes NMDA-type, AMPA-type, and metabotropic glutamate receptors.

1.1.2. Caged Neuromodulators

In addition to opening ion channels, neurotransmitters also trigger second messenger cascades by acting upon metabotropic receptors, thus influencing more than membrane potential. Since the signaling pathways triggered by metabotropic receptors are

not necessarily all identified, a logical approach is to employ caged receptor agonists.

For purposes of classification, we use the term “neuromodulator” to denote transmitters that have been traditionally thought to act more slowly than the millisecond-scale action of fast neurotransmitters such as glutamate. Physiological studies of neuromodulator action have employed agonists added to the bath or, at best, delivered in a pulsatile fashion to a targeted region of tissue through a micropipette or capillary tube. However, these modes of presentation may be far slower than the time scale of “modulator” action in vivo. The neurotransmitter/neuromodulator distinction has nearly disappeared with the appreciation of metabotropic actions of “fast” transmitters such as glutamate, GABA, and acetylcholine; conversely, neurons of the ventral tegmental area are now known to modulate dopamine levels in the nucleus accumbens on the time scale of 0.1 s (19, 20).

Many neuromodulators have been caged including agonists at 5-HT (21), adrenergic (22), and dopamine (23) receptors; for an exhaustive list, see (24). There are even caged peptide antagonists (25). Given the possibility of fast neuromodulator action in the CNS, emulation of neuromodulator activity by caged compounds is an attractive direction for future research.

1.1.3. Caged Second Messengers

A variety of intracellular signaling pathways can be controlled by light. Caged ATP was the first caged intracellular messenger for biological research (26, 27, 45) and has been used to study muscle contraction (28) and other cellular processes (29, 30). Another target for uncaging experiments is the calcium ion, which can be effectively caged by introducing calcium chelators that when photolyzed lead to a drop in affinity, thereby releasing calcium (31–35), or an increase in affinity, thereby buffering calcium (diaz-2; (36)). Calcium signaling has also been probed using caged IP₃ (37–39), caged cyclic ADP-ribose (40), a caged SERCA pump inhibitor (162), and caged caffeine (41).

Other caged messengers include caged nitric oxide (34, 42), BHC-caged cyclic nucleotide monophosphates (43), and caged nucleotides (38). Many older compounds are reviewed in (44). A number of new and old compounds are available from Molecular Probes (now Invitrogen), Calbiochem, or Tocris (Table 1 of (12)). Many caged molecules not commercially available can be synthesized relatively inexpensively. Compounds that have only been used in a few studies or made as a proof of principle may be difficult to obtain.

1.1.4. A Quantitative Index for Photoactivatability

To be useful in biological experiments, caged compounds must meet a number of basic criteria: good solubility, lack of biological activity such as interference with receptors or toxic effects, and rapid release of ligand upon illumination (for a review, see (45)).

In addition to these properties, one key parameter is sensitivity to photoactivation. In this regard, a useful quantity is the *uncaging index* U , defined for conventional (one-photon) absorption as $U = \varepsilon\phi$, where ε is the extinction coefficient (typically in units of $\text{M}^{-1}\text{cm}^{-1}$) and ϕ is the quantum yield, or the probability that a group will be photolyzed after absorbing a photon. The extinction coefficient ε varies as a function of illumination wavelength, but takes on very similar values for a given caged group, irrespective of the agonist that is caged. Quantum yield ϕ does not change with respect to wavelength as long as no other significant absorption bands are present, but does vary as a function of the identity of the caged molecule and the caging position. The higher the value of the uncaging index, the less light is needed to achieve uncaging. At a minimum, the light levels used to photolyze caged compounds should not damage or interact in unwanted ways with the biological system. This issue is especially important when using UV light, which is more likely to cause damage to the sample than visible or infrared (IR) light.

The relative merits of different cage groups are well-characterized quantitatively for caged glutamates but less so for other compounds. U values for some commonly used compounds can be found in (12, 31, 46). Also see Chap. 3 of this volume (Ellis-Davies).

1.2. Light-Sensitive Membrane Proteins

A major advance in recent years is the development and use of light-sensitive ion channels, pumps, and other signaling molecules. These proteins escape many problems associated with introducing caged compounds into neural tissue. They also carry the significant advantage of allowing targeted expression in subsets of cells using molecular methods. Light-activated channels and pumps have the potential to supplant caged neurotransmitters when the desired outcome is control of spiking in cells of a particular type.

1.2.1. Modification of Endogenous Channels

Endogenous ion channels can be made light-sensitive with chemical cofactor (48–54). A recent example is the SPARK channel, a Shaker potassium channel with a covalently attached ligand that causes the channel to open when illuminated. This channel can be exogenously expressed in mammalian neurons. A similar approach has been successful in creating a light-gated glutamate receptor, termed LiGluR (49, 50). Both SPARK and LiGluR require expression of the channel in the cell of interest followed by covalent modification. A technology that does not require exogenous gene expression is the photoswitchable affinity label (PAL) (51), which can be introduced into cells where it covalently attaches to an endogenous channel and renders it light sensitive (52, 53). This approach, reviewed in (54), is channel-specific and generally

does not require continuous illumination to keep the modified channels open. In addition, because it targets potassium channels, it may allow subtle modulations of neuronal firing (55).

1.2.2. Introduction of Exogenous Channels

A recent exciting advance in probing biological tissue with light is the development of “optogenetics,” the genetic expression of light-gated ion channels and transporters. The most widely used optogenetic molecule is channelrhodopsin-2 (ChR2), originally isolated from the green alga *Chlamydomonas reinhardtii*. ChR2 is a nonspecific cation channel and generates an inward (depolarizing) current (56) that can excite neurons on a time scale of milliseconds (57–59). ChR2 consists of the protein channelrhodopsin-2 (Chop2) with a covalently linked all-*trans*-retinal molecule that acts as the phototransducing moiety. In many types of vertebrate neural tissue, this channel functions in conjunction with the endogenous all-*trans* retinal that is naturally synthesized; in other preparations, all-*trans* retinal must be added to the system (58).

Upon blue-light excitation, the ChR2 channel opens to generate current within 1 ms. While the current-conducting photocycle of ChR2 is still not completely understood, it has generally been observed that sustained illumination of a ChR2 population beyond the initial peak amplitude leads to a smaller sustained current that reflects inactivation, light-dependent recovery to the initial light-excitable state, and reopening (i.e., multiple photocycles). Photocurrents decay to zero within ~10–100 ms of light offset depending on several experimental conditions, including pH (59–62). Between light-stimulation periods, recovery to the initial light-excitable state occurs more slowly than it does under illumination, imposing a delay between trials (~10 s) to repopulate the initial excitable state.

Engineered modifications to the photocycles of ChR2 and similar molecules have produced channels with different kinetics under sustained illumination, possibly favoring longer-lasting, larger-amplitude photocurrents from a photocycling population (60, 63). Other types of ChR2 molecules have been engineered to remain in a current-conducting state for much longer (up to ~100 s), allowing switchable step-like currents to be activated by blue-light excitation (64). Spectrally shifted absorption of this long-lasting current-conducting intermediate allows the termination of these currents upon illumination with green/yellow light. Another naturally occurring light-gated ion channel, comparable in several ways to ChR2 but with a red-shifted peak excitation wavelength, has been found by searching a genomic database by predicted functional homology (65).

Under full-field illumination, illumination power as low as 0.3 mW is sufficient to drive spiking in ChR2-expressing neurons (66), although 5–10 mW is often used (57, 67). In ChR2-based studies, where the desired physiological effect is often stimulation

of an action potential, one straightforward approach is to use a wide-field light source to illuminate all membrane-bound ChR2 molecules in a cell at once. Many microscopes configured for wide-field fluorescence imaging with an arc lamp can be modified at moderate cost for photostimulation experiments. Standard filter sets for imaging GFP fluorescence transmit excitation light to the sample that is near the peak wavelength for ChR2 excitation. To control the timing of illumination, fast shutters (e.g., Vincent Uniblitz VS35 shutter+VCM-D1 driver) can be introduced into the optical path, although the time required to open or close a mechanical shutter fully can, in some cases, impose a “fingerprint” on photocurrents.

An alternate approach that costs less and offers more precise temporal control over illumination is to use light from a high-power light-emitting diode (LED; e.g. LXHL-LB5C from Philips Lumileds). LEDs are available in a variety of wavelengths with narrow spectral bandwidths, and can be combined with inexpensive transistor-based gating circuits to switch light on or off very rapidly. LED illumination must be relayed to the sample with an appropriate optical configuration; for an example describing a substage configuration supplying LED-based Köhler illumination, see (68). For an excellent characterization of LEDs in general, see (69).

Inhibition is also possible using a chloride pump from *Natronomonas pharaonis*, halorhodopsin (NpHR) (70), which generates a hyperpolarizing current when excited by yellow light and can be used to inhibit neural activity in dissociated culture or intact tissue (71–73). As in the case of ChR2, variants and homologs have been developed for increased current amplitude, tolerability at high expression levels, and localization to the plasma membrane (eNpHR; (74)), or increased current amplitude and accelerated trial-to-trial recovery (75). eNpHR has recently been used in mammals to inhibit firing of targeted cells in vivo (76, 77).

It is worth noting that the sensitivity of channelrhodopsins and halorhodopsins to blue and yellow light, respectively, opens the possibility of bidirectional control of neuronal excitability using multiple-wavelength illumination by combining them with one another or with caged compounds.

For additional information, we refer readers to (73), Chap. 6 of this volume (Han and Boyden), and another excellent discussion of light-sensitive channels and other photosensitive molecules (78).

1.2.3. Engineered Light-Sensitive G-Protein- Coupled Receptors

Recently, it was demonstrated that the intracellular portions of rhodopsin may be altered to couple light absorption events to intracellular second messenger activity, thus placing G-protein receptor-coupled signaling under optical control (79). Two such engineered receptors, termed optoXRs, were constructed:

opto- α_1 AR, which mimics the intracellular actions of the α_{1a} adrenergic receptor (G_q recruitment leading to IP_3 production and calcium release from intracellular stores), and opto- β_2 AR, which mimics the intracellular actions of the hamster β_2 -adrenergic receptor (G_s recruitment leading to elevated cytosolic cAMP). Illumination of the opto- α_1 AR-expressing nucleus accumbens when mice were in a particular region of their enclosure produced a preference for that region on the following day.

2. Targeting of Photoactivatable Molecules

Photoactivatable molecules can be introduced into the experimental preparation in many ways. For caged neurotransmitters and neuromodulators, the principal options are bath perfusion (Sect. 3.1) and focal application through a capillary tube (Sect. 3.2). Caged intracellular ligands such as calcium and second messengers must be delivered by microinjection or via patch-clamp electrode, or else made membrane permeant by using AM esters to neutralize anionic moieties, an approach that is useful for delivering calcium chelators (80, 81). Exogenous proteins such as light-gated channels require expression systems (Sect. 3.3).

2.1. Bath Application

Bath application has the advantage of relative simplicity and produces uniform concentration of the compound throughout the bath. Commonly, in vitro experiments using caged compounds are done with caged compound solution pumped in a looped perfusion (82, 83). Recirculation uses less caged compound than a gravity-driven non-recirculating perfusion system.

2.2. Focal Application Through Capillary Tubing

Local pressure ejection of a caged compound solution has a number of advantages. First, the flow of the compound can be adjusted independently of the bath flow. This is particularly useful as a control to determine whether the caged compound itself affects biological function. Second, much smaller volumes are required, thus economizing on cost. For example, in our experience, an 8-h experiment using 15 mM of MNI-glutamate (\$150 for 10 mg, Tocris) will use less than 50 μ l of solution applied under 0.5 psi (34 mbar) through a 50- μ m inner diameter capillary tube. The resulting cost is less than \$4 per experiment. In contrast, a recirculating bath of 6 ml containing 2.5 mM of MNI-glutamate would cost \$72 and last less than half as long even under modest ambient light conditions.

Suitable capillary glass tubing of various diameters can be purchased from Polymicro Technologies. Tubing must be carefully scored and broken to a useful length using a ceramic cleaving stone (Polymicro) or a capillary cutter (Shortix, Scientific

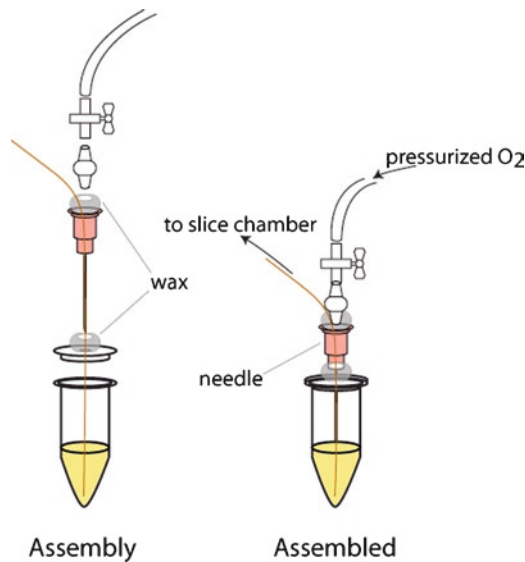


Fig. 1. Assembly of a low volume reservoir for focal elution of a caged compound solution into an experimental preparation. Bone wax is used to seal joints. The tube is covered in foil (not shown) to block room light.

Instrument Services, Inc.). A clean flat break prevents excessive turbulence of flow. A schematic for a simple pressure ejector is shown in Fig. 1.

2.3. Expression of Genetically Encodable Probes

2.3.1. In Utero Electroporation

Genetically encoded channels must be expressed within the cell of interest and then targeted to the membrane. Gene delivery methods include in utero electroporation of DNA, virus-based expression vectors, and the creation of transgenic animals.

Nucleic acids can be driven across cell membranes by strong electric fields. Several recent studies demonstrate the feasibility of electroporating transgene DNA into developing tissues (84, 85). In the brain, ChR2 has been expressed in specific layers of neocortex by prenatal electroporation to examine the functional targets of interhemispheric projections (86, 87). Electroporation can be done in utero, after which gestation can continue. One caution is that the voltages used to electroporate can damage developing tissue, leading to low viability depending on the position and geometry of the target tissue and electrodes.

2.3.2. Viral Vectors

Transgenes may be inserted into viral vectors and injected directly into tissues of interest. The simplest type of application of this method is stereotactic targeting of viral particles to a structure of interest (88) such as the mouse hypothalamus (89). In intact

brain tissue, lentiviruses (90), adeno-associated viruses (91, 92), and herpes viruses (93, 94) have found wide use. Retrograde interhemispheric transport of a herpes virus expressing ChR2 has been used to identify contralaterally projecting cortical cells in the intact brain by illuminating during in vivo electrophysiological recordings (95). To enhance the specificity of virally delivered transgenes, injection of viral vectors may be performed in a cell-specific Cre-expressing mouse line (77, 96–99). In some recent applications (77, 98, 99), a double-floxed inverted strategy (100) was used to activate the transgene by inversion between two pairs of flanking *lox* sites rather than by excision of a STOP sequence. This increased the specificity of expression, and allowed tests of the causal role of dopamine neurons (98) and parvalbumin neurons (77, 99) in circuit performance and behavior. Finally, functional circuits may be infected by viruses that are able to cross synapses. References (101) and (102) provide comprehensive reviews of virus technology in neuroscience.

2.3.3. Transgenic Animals

Making a transgenic animal (103, 104) combines the spatial and temporal specificity of regulated gene expression with the possibility of having a continuous supply of experimental animals. Powerful genetic tools now allow the restriction of transgene expression by temporal and functional boundaries. For example, a transcriptional stop sequence may be “floxed” (flanked by *loxP* sites) and inserted between a transgene and a strong universal promoter. The transgene may then be activated in specific tissues or cell types by the action of Cre, a site-specific DNA recombinase that excises the material between the *loxP* sites. This Cre-*lox* system may be used to produce particular profiles of transgene expression by crossing a floxed mouse with a cell type-specific Cre line, so that the transgene will be expressed in the tissues at the intersection of the two distributions. Reversible temporal control of transgene expression is also possible using, for example, “tet-ON” and “tet-OFF” systems (105). References (106) and (107) provide comprehensive reviews of genetic methods and their use to target neuronal subtypes.

Problems associated with the transgenic approach include the long lead time required to generate an organism successfully, uncertainty as to what cell types will express under the chosen promoter, and the possibility that expression will eventually be silenced over multiple generations by epigenetic mechanisms. In addition, at present, transgenesis is possible only in selected model organisms.

Several ChR2 transgenic animal lines are currently available. ChR2-expressing mice driven by the *thyl* promoter (108) are available from Jackson Laboratories. ChR2 and NpHR have also been introduced into the translucent nematode *C. elegans* (73, 109).

Efforts are also underway to achieve cell-type specificity for any transgene using conditional and combinatorial expression systems.

3. One-Photon Versus Two-Photon Excitation

Caged compounds are typically excited by near ultraviolet (UV) light (330–400 nm), which is strongly scattered by brain tissue, leading to limited depth penetration (110) and degradation of the focus. Also, single-photon methods do not provide a way to restrict excitation to a single Z-focal plane, so molecules away from the plane of interest may also be excited. The major advantages of two-photon excitation (TPE) are decreased heating by light absorption a more localized excitation spot due to reduced scattering by IR light, and an intrinsic “optical section” around the plane of focus (111).

3.1. Cost Considerations

For one-photon uncaging of glutamate, in our laboratory we use a frequency-tripled Q-switched Nd:YVO₄ laser (355 nm, DPSS Series 3501). Considerably less expensive sources of UV and near-UV light include solid-state UV lasers (e.g., Oxixius Violet), flash lamps (112, 113), and UV LEDs (available from Nichia Corporation, Japan; (114–116)).

Relative to UV, the major disadvantage of pulsed IR TPE is the cost of the excitation source. Fixed-wavelength femtosecond pulsed IR lasers suitable for two-photon uncaging are available from, e.g., Del Mar Photonics (California, USA) and Femtolasers, Inc. (Massachusetts, USA). Much more commonly used wavelength tunable IR lasers confer flexibility but are more expensive (e.g., Newport/Spectra-Physics or Coherent). The need for TPE can sometimes be obviated by careful choice of the preparation geometry, or by targeted application or expression of photoactive molecule.

3.2. Chemical Two-Photon Uncaging

One simple way to improve the characteristics of any uncaging system is to add a second inactivating group to the molecule of interest (117). Production of active agonist then requires two photolysis events, introducing a nonlinearity by making the probability of photolysis proportional to the second power of light density. Out-of-focus uncaging is reduced since, as in the case of true two-photon uncaging, active ligand molecules will be preferentially produced in the volume where light density is maximal. This approach has been termed “chemical two-photon uncaging” (117).

In principle, the use of chemical two-photon uncaging produces an increase in spatial resolution comparable to that provided by conventional two-photon uncaging, without the significant cost of a pulsed IR light source. Instead of requiring a pulsed laser, chemical two-photon uncaging only requires the excitation events to occur within a few milliseconds, the time scale on which a molecule that has been uncaged once remains in the focal volume.

Confinement of the photolysis volume is important for extracellular uncaging of neurotransmitter in brain slices, since it limits the action of the uncaged molecules on the cells located above and below the focal volume. However, this approach still uses UV light, limiting its usefulness to the most superficial $\sim 50\ \mu\text{m}$ of brain slices (110). In addition, over repeated uncaging pulses, partial photolysis products may accumulate, though this can be reduced by the use of a local perfusion (see Sect. 3.2).

An important advantage of double caging is that it can reduce the background activity of a caged compound by making it less similar in structure to the native agonist, reducing the risk of undesired interaction with biological targets (118). Also, handling is easier since the requirement of two uncaging events makes the production of free agonist by room light or spontaneous degradation less likely. Multiple-caged compounds are generally not commercially available, but their synthesis is simplified by the fact that the design of single-caged compounds usually involves the identification of multiple caging sites. For example, the synthesis of double-caged IP_3 is achieved most simply by synthesizing triple-caged IP_3 and “photolyzing back” to the double-caged form (118).

3.3. Spot Size

A highly localized excitation spot is not always optimal. For any scanning system (as opposed to a holographic or other scanless system; see Sects. 6.4 and 6.5), a reduced spot size reduces the simultaneously excitable area. For example, an extended portion of a dendritic arbor or dendrite cannot be simultaneously illuminated with a diffraction-limited spot. In cases where spine-level spatial resolution is not necessary, a larger spot size may in fact be desirable, and may be obtained by using a flash lamp or by introducing a spatially diffuse UV laser beam, e.g., through a multimode fiber (119). For focused laser light the region of concentrated photoactivation near the focus may be expanded by using a lower numerical aperture lens or by underfilling the back aperture of a high-numerical aperture objective (120).

3.4. Absorption Spectrum of Molecular Target

A molecule’s peak wavelength for two-photon absorption is often nearly twice the peak wavelength for one-photon absorption; however, this is not always the case (111), and both spectral

sensitivity and absolute absorptivity must generally be determined empirically. Two-photon absorptivity (121) is usually reported in terms of the two-photon absorption cross-section, typically expressed in Göppert-Mayer units ($1 \text{ GM} = 10^{-50} \text{ cm}^4 \text{ s/photon}$), or action cross-section (quantum efficiency \times absorption cross-section, also often reported in units of GM). Rhodamine 6G is considered to have a large action cross-section, $\sim 150 \text{ GM}$ (122). The action cross-section of caged glutamate reached a usability threshold of 1 GM with the synthesis of the BHC (4) and MNI (5) caging groups, leading to the rise of two-photon glutamate uncaging (82, 123). Two-photon absorption cross-sections have not yet been measured for a large number of less commonly used cage groups, such as those which have been used to cage GABA and most of the compounds listed in Sect. 2.2.

3.5. Two-Photon Excitation of Light- Activated Channels

Unlike caged compounds, which may be synthetically designed to possess high two-photon excitabilities, the two-photon excitability of light-gated ion channels depends in part on the light-absorbing properties of the intrinsic chromophore (all-*trans* retinal). The one- versus two-photon excitabilities of light-gated proteins, as determined by the properties of the chromophore and by the photocycle dynamics described in Sect. 2.2.2, are only beginning to be explored.

One investigation has described the spectral sensitivity of ChR2 responses under TPE, using optical detection of fluorescence transients associated with a calcium-binding dye to infer photocurrent amplitudes (124). More recent electrical recordings of ChR2 currents stimulated with low-power TPE (125) give a cross-section of 260 GM and demonstrate single action potential triggering using TPE.

4. Beam Steering: Introduction

In order to activate photosensitive molecules for neurophysiological experiments, it is often necessary to have precise control over the timing and location of illumination. In the remainder of this chapter, we discuss technologies for producing patterned illumination.

To illuminate areas comparable in size to the field of view, a focused beam is unnecessary and a flash or an arc lamp may be used (see (126) for a discussion). For micron-scale spatial resolution, a focused beam must be introduced. Here we concentrate on the case in which the activating light comes from a laser and is directed through the microscope objective. An alternate

approach, the use of an adjacently positioned optical fiber, removes some difficulties of power loss and chromatic aberration by the microscope objective, at the expense of some spatial resolution (126).

For some experiments, beam steering may not be required. By aligning the structure of interest with a single photolysis point, it is possible to interrogate optically a single substructural element with fine temporal resolution (38). Such an arrangement has been successfully combined with the use of a motorized stage, adjusted slowly between trials, to map responses to photorelease over a wide area, as long as time is not an issue (127–131). Where only one site of activation is needed, an alternate approach with potentially superior spatial and temporal resolution is iontophoresis of agonist (132).

In most experiments, imaging is necessary in order to locate the site of photoactivation. In the simplest case, an image can be generated using a CCD camera on a conventional microscope. However, frequently both the manipulation (photoactivation) and the measurement (imaging) require a steered beam. This situation places additional constraints on the technologies that can be used; at the very least, some technical expertise/hardware is required to coordinate the two processes.

In the final two sections of this chapter, we will examine the pros and cons of technologies for achieving sophisticated spatial and/or temporal control. We will first review technologies that have already been used to answer questions in neurophysiology at the time of this writing (Sect. 6). The issues and choices to be discussed when selecting from mature technologies are outlined in Fig. 2. In Sect. 7, we review more advanced technologies that we expect to become more accessible in the near future. In both sections, we will use the term “*XY* scanning” to refer to beam steering within a horizontal plane and “*Z* scanning” to refer to beam steering to points at varying depths in the specimen.

All beam shaping and steering technologies need to take into consideration the potential for aberration. Chromatic aberration can especially complicate photoactivation experiments since optical components are less likely to be corrected for IR or UV wavelengths than visible wavelengths. This leads to potential registration errors between photoactivation and imaging, especially in the *Z* direction (110). Many objective lenses are now corrected for commonly used wavelengths, but this must always be tested empirically. Moderate axial errors can be corrected by diverging or converging one of the wavelengths in order to displace the focus axially (133). Correction strategies for dispersive elements, which broaden femtosecond near-IR pulses, are discussed in Sect. 7.

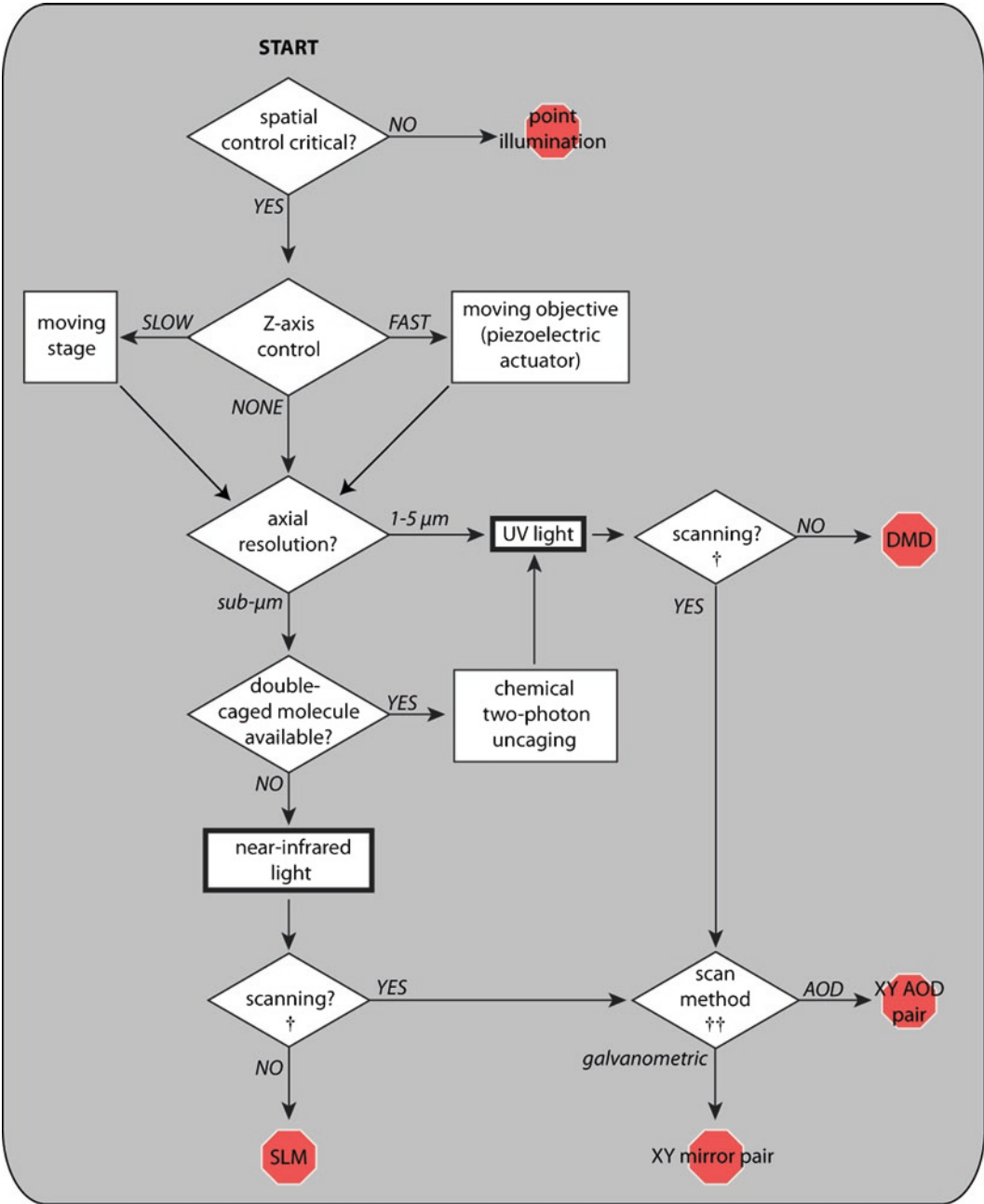


Fig. 2. Flowchart for selection of photoactivation technology. Abbreviations: *AOD* acousto-optic deflector, Sects. 6.2, 6.3, and 7.1; *DMD* digital micromirror device, Sect. 6.4; *SLM* spatial light modulator, Sect. 6.5. †Scanning (see Sect. 6.4 for an explanation of the advantages and disadvantages of scanless beam shaping). ††Scan method (see Sect. 6.3 for a comparison of galvanometric and AOD-based scanning).

5. Beam Steering: Current Technologies

5.1. *XY Scanning with Mirrors Mounted on Galvanometric Scanners*

Mirrors several millimeters in size, mounted on galvanometric scanners, are the standard approach to scanning microscopy (134, 135). When used to uncage neurotransmitters, galvoscanning technology has allowed groundbreaking studies of dendritic integration (123, 132, 136). Today, such technology is commercially available as components (Cambridge Technology, Massachusetts, USA), or in complete systems such as the Ultima IV from Prairie Technologies, which features one set of scanning mirrors for two-photon imaging and another set (requiring a second IR laser) for two-photon uncaging.

Newer microscope designs have gone beyond the raster scan pattern that has characterized most two-photon imaging to achieve higher visitation speeds with scanning mirrors (137). This has allowed fluorescence signal acquisition from locations separated by up to several millimeters, allowing the imaging of large networks (138). These methods are applicable to photoactivation. In principle, any scan geometry that maintains the minimum single-location exposure time necessary for sufficient photoactivation (\sim tens of μ s) is acceptable. For example, uncaging could be done by using a spiral trajectory (X and Y sinusoids) (139) with discretization of locations achieved by blanking the beam with an electro-optic modulator (EOM) between spots. To date, most photoactivation studies have used scanning mirrors to traverse locations on a single dendrite at up to 3,000 Hz.

5.2. *Acousto-Optic Deflectors*

Perhaps the most rapidly developing technology for beam-steering applications is the acousto-optic deflector (AOD), which allows inertia-free scanning. The heart of an AOD is a crystal that behaves like a tunable diffraction grating with a grating constant that can be adjusted by varying the frequency of a sound wave propagating across the crystal, generated by a piezoelectric transducer interfaced with the crystal. AODs may be set up to direct most ($>50\%$) of the input beam intensity into the first-order diffraction peak, generating a movable beam that may traverse a range of angles determined by the frequency bandwidth available to modulate the propagating sound wave. The deflected beam is mapped to a specific location in the preparation with appropriate relay optics. One AOD is required for each dimension of the coverage area.

5.2.1. *The Spatial Resolution of an AOD-Based System*

The number of resolvable points in the sample plane is determined by the number of resolvable angular deflection angles provided within the range of the scanning element. For a given range of angles $\Delta\theta$, a beam with an intrinsic divergence angle ϕ can occupy N resolvable angular locations, i.e.,

$$N = \frac{\Delta\theta}{\phi}. \quad (1)$$

For an AOD-based scanner, the range of deflection angles depends on the beam wavelength λ , the bandwidth of the driving acoustic frequency, Δf , and the velocity of sound in the AOD crystal medium, V :

$$\Delta\theta = \frac{\lambda\Delta f}{V}. \quad (2)$$

The divergence of the beam, ϕ , is approximated (for a uniformly illuminated aperture) by dividing the beam wavelength by the beam diameter, which for AOD-based scanners is limited by the deflector aperture size D :

$$\phi = \frac{\lambda}{D}. \quad (3)$$

Substituting Equations (2) and (3) into Equation (1) and simplifying gives the number of resolvable spots, N , in terms of the acoustic propagation time across the crystal Δt :

$$N = \Delta f \Delta t. \quad (4)$$

This quantity is sometimes referred to as the time–bandwidth product. In the case of a Gaussian beam that does not fill the aperture uniformly, N is an overestimate of the true performance. The most notable trade-offs are between spot size and scanning rate, and between bandwidth and number of resolvable spots (140). Increasing D , for example, requires less beam expansion to maintain a full back aperture and, therefore, allows more resolvable points. A useful calculator for examining design trade-offs can be found at the website of MolTech GmbH (http://www.mt-berlin.com/frames_ao/acousto_frames.htm). The ongoing development of AODs with larger apertures (e.g., 13 mm, (141)) promises to increase the field of view and the number of resolvable points available with this scanning method.

TeO₂ crystals are particularly well suited for scanning applications with AODs. TeO₂ possesses a high figure of merit with a slow acoustic velocity, conferring upon it high deflection efficiency, high resolution, and a large scan angle for a relatively low RF bandwidth. TeO₂ transmits effectively over a wide spectral range including both IR and near-UV. For UV applications, screening individual crystals for custom selection is advisable for maximum efficiency (110). For pulsed IR applications, the spectral bandwidth of optical pulses leads to dispersion; pulse dispersion compensation is often used to restore original optical pulse properties (see Sect. 7.1.1). AODs are available commercially from many

sources (e.g. Isomet, Brimrose Corporation, Noah Industries, and Crystal Technology Inc.).

5.2.2. *XY Scanning with Two Crossed AODs*

Two perpendicularly oriented AODs may be used to scan an *XY* plane. In this case, if the input beam fills or nearly fills the AOD aperture, an additional limit on scan angle appears due to vignetting at the second AOD aperture. To transmit all deflection angles from the initial (*X*) deflector through the aperture of the second (*Y*) deflector (allowing the maximum scan angle and hence the maximum addressable area), the two deflectors can be placed in close physical apposition (for this reason, *XY* pairs are often sold as a unit) or angular deflections from the first crystal's exit aperture can be optically relayed to the face of the second (142).

For patterned photoactivation with UV light in our laboratory (110), we use a Brimrose TeO₂, model 2DS-150-50-0.364, which contains two AODs with 7-mm apertures, driven by command signals from a two-channel variable frequency driver (VFE-150-50-V-B1-F2-2CH). With these parameters, we are able to visit up to 20,000 locations per second stably and reproducibly, accessing many sites in a brain slice virtually simultaneously (for example, mimicking simultaneous parallel fiber inputs to visually identified regions of a Purkinje cell dendritic arbor, dynamically adjustable from tens to hundreds of μm^2 in size). With this system, we are currently exploring the role of synchrony in branchlet-level dendritic excitation in cerebellar Purkinje neurons (Fig. 3).

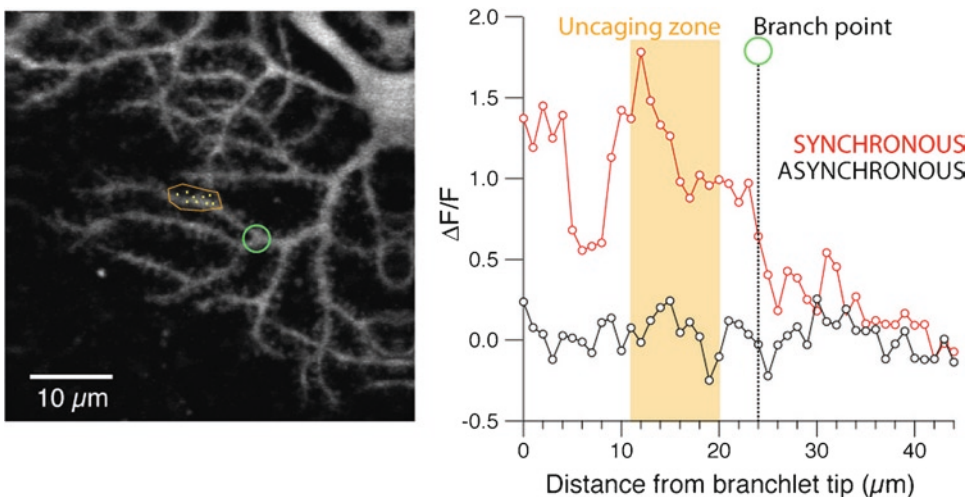


Fig. 3. Spatial structure of branchlet-level calcium transients evoked by synchronous glutamatergic input to a Purkinje cell. *Left*: Stimulus points indicated by *yellow dots*. *Right*: One-dimensional profile of calcium response to synchronous (50 μs between points) and asynchronous (10 ms between points) input (Civillico and Wang, unpublished).

5.3. XY Scanning

Comparison:

Galvanometric

Scanners Versus AODs

The choice between AOD-based and galvanometric scanning involves a trade-off between addressing speed (where AODs are preferred) and range (mirrors). For an AOD-mediated beam deflection, the travel time between two scanned points is determined by the propagation time of sound across the beam diameter at the crystal, usually tens of microseconds. This makes any two arbitrarily spaced points within the scan area accessible within one switching time. However, AODs provide deflection over a more limited range of angles (typically ~ 50 mrad), while galvanometric mirrors typically span hundreds of milliradians. This disadvantage can be partially, though not completely, compensated for by choosing a lens system (see Fig. 4) that increases the angular range at the objective.

Figure 4 illustrates some of the relevant spatial relationships. In the paraxial limit, the relation between an angular beam deflection from the optical axis at the back aperture of an objective lens θ_{obj} , and the lateral displacement in the plane of focus x , is

$$x = f_{\text{obj}} \theta_{\text{obj}}, \quad (5)$$

where f_{obj} is the focal length of the lens. The focal length f_{obj} is related to the objective magnification M by

$$f_{\text{obj}} = \frac{L}{M}, \quad (6)$$

where L is a manufacturer-specific tube lens focal length (e.g. 180 mm for Olympus objectives). The deflection angle θ_{obj} is related to the deflection angle θ_{scan} at the scanner by the beam expansion factor of the focal telescope between the scanner and objective E :

$$\theta_{\text{obj}} = \frac{\theta_{\text{scan}}}{E}. \quad (7)$$

Substituting Equations (6) and (7) into Equation (5) gives the relation between scan angle θ_{scan} and lateral displacement at the focus as a function of beam expansion and objective magnification:

$$x = \frac{L}{M} \frac{\theta_{\text{scan}}}{E}. \quad (8)$$

This equation can be used to determine the available scanning range based on the maximum deflection angle produced by an AOD or galvanometric-based system. Otherwise, in cases where galvoscaning may be superior due to its wider range, the temporal/inertial limitations must be worked around, for example, by rational scan design (138).

As the technology advances, maximum available AOD aperture sizes are increasing, increasing the number of resolvable

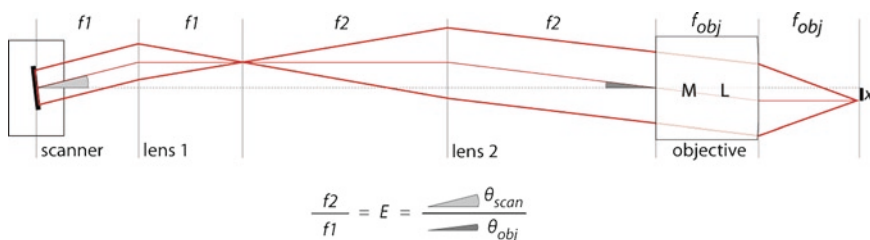


Fig. 4. Geometric optics of a one-dimensional scanning system. The scanner's pivot point is relayed to the back focal plane of the objective lens by a telescope (1:2 beam expansion in this example). The objective lens magnification (M) and reference tube length (L) determine the lateral offset x in the sample plane for a given value of θ_{obj} .

points and, with appropriate changes to the relay optics, enabling larger fields of view, at the cost of an increase in switching time. Note that while galvanometric scanners can produce deflections much larger than current AODs (hundreds of milliradians versus ~ 50 milliradians), the allowable angular range for a galvoscaning system is limited practically by the effective numerical aperture of the scan lens and by the acceptance angle of the objective (143).

5.4. Digital Multimirror Device

Methods that selectively illuminate different regions of the sample without beam-scanning deflection are said to be “scanless.” The most mature scanless technology at this time is digital micro-mirror device (DMD) technology, a rectangular array of mirrors each approximately $100 \mu\text{m}^2$ in size (e.g., a 10.5×14 mm chip, with $1,024 \times 768$ pixels; DMD-4000, Texas Instruments). Each mirror can be switched independently between two positions to deflect incident light selectively into the experimental preparation. Mirror movement is fast ($\sim 40 \mu\text{s}$) and digitally controlled, allowing complex simultaneous multispot excitation patterns to be rapidly modulated. The principal disadvantage of DMD technology is that patterns are created by deflecting light out of the optical path. This limitation can be worked around by starting with a higher power light source. In an optical configuration for a neurophysiological experiment, an image of the illuminated DMD surface would be relayed to the sample plane. If coherent light is used, it must be scrambled to eliminate speckle with, for example, a vibrating mirror.

For example, compare the illumination control obtained with, e.g., a DMD-4000 to that obtained from a scanning configuration. Consider an optical setup consisting of a $\lambda = 355$ nm Gaussian beam incident upon an 8 mm wide DMD focused through a $40\times$ objective with an NA of 0.8. The projected image is $200\text{-}\mu\text{m}$ wide in the sample plane. The light energy delivered is distributed over all the mirrors that project to this region. In contrast, in the scanning case, all of the beam power is concentrated in a spot approximately 280 nm in the lateral

direction assuming a diffraction-limited focus, giving a density of approximately 500,000 times more energy per μm^2 than the DMD case. This reduced power per unit area dictates that a higher-energy light source will be required relative to a scanning configuration. Because each mirror represents a point, laser illumination is unnecessary and a flash lamp may increase the amount of light energy available.

Current DMD models from Texas Instruments are available in configurations optimized for UV or visible light in which the window in front of the mirror array is coated for high transmission at different wavelengths. In practice, the UV-optimized coating enhances UV transmission by about 10%. This technology is not ideal for TPE because of the power loss described above, as well as the fact that the manufacturing process involves coating the mirrors with aluminum rather than a dielectric coating, making them relatively poor reflectors of near-IR wavelengths. For these reasons, DMDs are most useful for one-photon excitation of molecules activated by visible or UV wavelengths.

Investigators using DMD technology report that the greatest expense, in terms of time and cost, is the development of software controls. DMD control may be simplified with third-party add-on modules such as the accessory light packages (ALPs) supplied by Vialux (Germany) that provide on-board memory and facilitate synchronization and display of mirror sequences, enabling the loading of temporal sequences onto the DMD chip which can then be delivered at the maximum display rates of 16–32 kHz, depending on the chip model. A set of tools written by Dr. Nicholas Hartell of the University of Leicester to control the ALP/DMD-3000 is available as an extension to Igor Pro (Wavemetrics, OR).

5.5. Holographic Beam Shaping with a Spatial Light Modulator

Another scanless technology for generating XY patterns is a liquid crystal spatial light modulator (SLM), which is a display that can be programmed to modulate the phase of the photoactivation beam to produce a desired intensity pattern at the focal plane. When the phase mask is suitably chosen, generally by an iterative algorithm (144), a beam reflected from the SLM will be shaped into a hologram, i.e., the phase of the light is modulated so that the highest intensity regions in the focal plane are arranged to produce an illumination pattern of arbitrary shape and size. A recent study (145) has demonstrated the utility of this approach for UV uncaging over subcellular regions defined “on the fly.” The SLM can generate many spots with true simultaneity, and even has the ability to generate diffraction-limited spots over a 50- μm Z-focal range above and below the focal plane (V. Emiliani, personal communication).

In some cases, this technology is suitable for spatially patterned TPE. A recent study has demonstrated that an SLM can be used to generate arbitrarily patterned TPE and that superimposing

“lens functions” on predefined phase masks confers some control over the Z -focal dimension of the excitation (146). Currently, the refresh rate for an SLM is limited to tens of Hz.

Holographic illumination patterns generated by spatial light modulators may include “ghost spots” of unwanted light. To eliminate unwanted photoactivation by these spots, an SLM may be combined with the use of a DMD as a dynamic spatial filter to increase the contrast of complex holographic patterns (C.-M. Tang, personal communication).

5.6. Z-Scanning

5.6.1. Slow Z-Scanning with a Moving Stage

Control of illumination in the Z -dimension, or axially resolved photoactivation, can be implemented most simply by controlling the distance between the microscope objective and the sample using a stepper motor coupled to the focusing knob of the objective, or a motorized stage to move the sample. Objective positioning schemes are employed in popular programs for controlling two-photon microscopes, including CfNT (R. Stepnowski, Bell Labs, and M. Müller, Max Planck Inst. Med. Res.) and ScanImage (147). While such approaches are suitable for collecting a series of images in sequence (e.g., to reconstruct cell morphology), they are not optimized for manipulating the plane of focus on neurophysiological time scales (e.g., for multisite photoactivation).

5.6.2. Faster Z-Scanning with a Piezoelectric Actuator

Rapid control of the Z -focal plane of an activating beam may be achieved by driving an oscillating piezoelectric actuator to modulate the Z -focal position of the objective. Actuators from Physik Instrumente (Germany) have found use in the imaging of neuronal and glial activity (139, 148) and could be adapted for targeted photoactivation. They may be conveniently added on to many common microscope builds, including the complete system sold by Prairie Technologies. The displacement of the objective is a function of the applied voltage; converter boxes and PC interfaces are available that allow the objective to be driven by an arbitrary waveform. In practice, inertia of a moving objective requires a smooth trajectory such as a sinusoid for fidelity to the command signal. The position of the objective can be combined with the known positions of XY scanning elements to reconstruct a three-dimensional scan path (139); the same approach could be used to produce a three-dimensional photoactivation trajectory.

6. Beam Steering: Emerging Technologies

Here we describe several state-of-the-art beam-steering technologies. While these methods are being developed in the context of imaging, they are amenable to use in photoactivation as well.

6.1. Pushing the Envelope with AODs

6.1.1. Two-Photon Excitation with AODs

Two-photon scanning systems using AODs for beam steering have recently become feasible. The principal optical limitation to be overcome is the dispersion of ultrashort laser pulses as they pass through an AOD. Ultrashort pulses are necessarily composed of a range of wavelengths that will travel at different speeds through typical AOD crystal materials, and be diffracted to different locations (see Equation (3) above; see (141)), resulting in pulses that are broadened temporally and spatially.

Pulse broadening may be compensated by adding dispersion to the laser pulses that is equal in magnitude and opposite in sign to that introduced by the AOD(s), for example, with a temporal pre-chirper composed of a pair of prisms (149, 150) or with a diffraction grating or acousto-optic modulator (AOM) (AA Optoelectronic, Orsay, France; (141, 150)). Spatial and temporal dispersion may be compensated simultaneously with a single tilted prism (151) placed at the correct distance from a pair of crossed AODs. The need for dispersion correction may be reduced by the use of slightly longer laser pulses.

6.1.2. Lensing with AODs

Rather than stepping the drive signal to a series of constant frequencies as for XY scanning (Sect. 6.2.2), lensing may be achieved by continuous modulation of the driving frequency to an AOD. Driving an AOD with a linear frequency sweep produces a continuously varying diffraction grating constant across the crystal face, resulting in a convergent or divergent beam and a fixed axial displacement of the focus that is proportional to the rate of change of the frequency. At the same time, however, the frequency modulation produces continuous lateral displacement of the focus (see Equation 2). To maintain independent control along one lateral dimension while directing the focus axially, the beam must be directed through a pair of AODs driven by counterpropagating frequency chirps (152, 153). In this configuration, the offset between the chirp center frequencies determines the lateral position, while the chirp rate determines the axial position as before. In this way, an AOD pair driven by counterpropagating frequency chirps functions as a cylindrical lens; two orthogonal pairs function as a spherical lens.

The allowable bandwidth for the driving frequencies constrains the addressable volume as follows: Because the axial displacement in Z depends on the chirp range while the lateral displacement in X or Y depends on chirp offset between the members of the X or Y pair, respectively, larger axial excursions (wider chirp range) require smaller lateral excursions (smaller distances between chirp centers) in order to fit within the allowed bandwidth. For this reason, the volume addressable by a 4-AOD scanner is octahedral, with the maximum XY span at $Z = 0$.

Using four AODs, a system has been demonstrated with axial and lateral scan ranges of 50 and 200 μm , respectively, at 60 \times magnification (142). With this system, calcium transients could be recorded in three dimensions from hippocampal CA3 cells. The investigators suggest that axial and lateral ranges of 200 and 350 μm , respectively, are possible with this technology. The addressable volume is primarily limited by the acceptance angle of the AOD crystals; wider acceptance angles (154) will further improve this method in the near future. Acquisition rates up to tens of kilohertz are possible, giving comparable time resolution to an XY -only AOD-based scanning system, with the advantage of motion along the Z -axis. Note that the use of four AODs allows x , y , and z positioning without moving the objective. These two independent effects allow for any scan trajectory within the addressable volume, within the limited acoustic bandwidth shared by the axial and lateral displacement signals.

A recently developed system makes use of four custom-designed AODs (163). The custom-designed AODs have an optically rotated crystal orientation, and the second AOD of each X and Y pair has a narrow transducer, which results in a wide acceptance angle to the curved wavefront from the first AOD of each pair. This results in a larger overall scan volume. With a 0.8 NA, 40 \times objective, the AOD scanner can focus over a >100 μm range. The custom AODs are much thinner than standard scanning AODs, reducing the temporal dispersion of the AODs sufficiently to enable a prism-based pre-chirper to compensate for temporal dispersion of the ultrashort laser pulses. This enables low-noise two-photon images to be obtained at much lower powers than without a pre-chirper. These design features allow random access point measurements in three dimensions at rates up to 30 kHz throughout an octahedral volume beneath the microscope objective.

The innovative neurospy project (155) achieves three-dimensional scanning with two AODs and a custom-designed Yb: KYW laser emitting long (310 fs) pulses in the 1,030-nm range. The longer pulse duration reduces spatial and temporal dispersion by the AODs. The two AODs can be used either as a single-plane XY scanner as described in Sect. 6.2.2 (each position specified by one frequency pair), or to implement a three-dimensional scan path (chirped driving signals). Relative to the 4-AOD systems described above, elimination of one AOD of each pair sacrifices some flexibility in the trajectory because axial displacements are coupled to particular lateral displacements. This system can be constructed at a fraction of the cost of other scanning systems and can be run entirely from a LeCroy Waverunner 64xi oscilloscope. Documentation, instructions, and software for the construction and operation of this “open-source” system are available at <http://www.neurospy.org>.

6.2. Temporal Focusing

By introducing geometrical dispersion of ultrashort laser pulses outside the objective focal plane, for example, with a diffraction grating, it is possible to create a temporal focusing effect, in which a spatiotemporal light pattern derived from an ultrashort pulse is temporally as it propagates through a volume, compressed at the temporal focal plane, and dispersed again as it propagates further. Temporal focusing is the converse of the spatial focusing employed in conventional TPE; instead of a spatially restricted, temporally extended focus, there is a spatially extended, temporally restricted focus. Temporal focusing has been demonstrated for depth-resolved two-photon imaging without scanning (156), and has recently been combined with SLM-based holographic illumination to enable the placement of an arbitrarily shaped photoactivation region with 5 μm resolution at the focal plane of the objective (157).

6.3. Other Methods

Additional three-dimensional imaging methods show promise for future use in targeted photoactivation but are still in early stages of development. Rather than moving the objective, a variable-focus lens employing a fluid-filled cavity (158) might be used to adjust the focal plane dynamically. A membrane-deformable mirror could be used for this purpose ((159, 160); e.g., Flexible Optical B.V., The Netherlands). A recent study (161) provided a remarkable demonstration of three-dimensional scanning using XY scanning with a pair of AODs, as described in Sect. 6.2.2, to direct a beam into the ends of a matrix of single-mode optical fibers, one fiber per desired imaging spot. By micropositioning the exit ends of the fibers, imaging spots could be positioned within a three-dimensional volume as desired. Target points were defined by a three-dimensional image reconstruction that was acquired with a parallel mirror-based scanning system.

Acknowledgments

We thank Karl Deisseroth, Valentina Emiliani, Jonathan A.N. Fisher, Mark McDonald, Ashlan Reid, Angus Silver, Cha-Min Tang, Stephan Thiberge, and Dejan Vučinić for helpful discussions and comments on this chapter.

E.F.C. is supported by a Robert Leet and Clara Guthrie Patterson Postdoctoral Fellowship in Brain Circuitry. J.P.R. is supported by a National Science Foundation Graduate Research fellowship. S.S.-H.W. is a W.M. Keck Foundation Distinguished Young Investigator and is supported by National Institutes of Health grant NS045193 and the National Science Foundation.

References

1. Walker JW, McCray JA, Hess GP (1986) Photolabile protecting groups for an acetylcholine receptor ligand. Synthesis and photochemistry of a new class of *o*-nitrobenzyl derivatives and their effects on receptor function. *Biochemistry* 25:1799–1805
2. Milburn T, Matsubara N, Billington AP, Udgaonkar JB, Walker JW, Carpenter BK, Webb WW, Marque J, Denk W, McCray JA et al (1989) Synthesis, photochemistry, and biological activity of a caged photolabile acetylcholine receptor ligand. *Biochemistry* 28:49–55
3. Wilcox M, Viola RW, Johnson KW, Billington AP, Carpenter BK, McCray JA, Guzikowski AP, Hess GP (1990) Synthesis of photolabile precursors of amino acid neurotransmitters. *J Org Chem* 55:1585–1589
4. Furuta T, Wang SS, Dantzer JL, Dore TM, Bybee WJ, Callaway EM, Denk W, Tsien RY (1999) Brominated 7-hydroxycoumarin-4-ylmethyls: photolabile protecting groups with biologically useful cross-sections for two photon photolysis. *Proc Natl Acad Sci U S A* 96:1193–1200
5. Canepari M, Nelson L, Papageorgiou G, Corrie JET, Ogden D (2001) Photochemical and pharmacological evaluation of 7-nitroindolyl- and 4-methoxy-7-nitroindolyl-amino acids as novel, fast caged neurotransmitters. *J Neurosci Methods* 112:29–42
6. Matsuzaki M, Ellis-Davies GCR, Nemoto T, Miyashita Y, Iino M, Kasai H (2001) Dendritic spine geometry is critical for AMPA receptor expression in hippocampal CA1 pyramidal neurons. *Nat Neurosci* 4:1086–1092
7. Papageorgiou G, Corrie JET (2000) Effects of aromatic substituents on the photocleavage of 1-acyl-7-nitroindolines. *Tetrahedron* 56:8197–8205
8. Gee KR, Niu L, Schaper K, Hess GP (1995) Caged bioactive carboxylates. Synthesis, photolysis studies, and biological characterization of a new caged *N*-methyl-D-aspartic acid. *J Org Chem* 60:4260–4263
9. Niu L, Gee KR, Schaper K, Hess GP (1996) Synthesis and photochemical properties of a kainate precursor and activation of kainate and AMPA receptor channels on a microsecond time scale. *Biochemistry* 35:2030–2036
10. Huang YH, Muralidharan S, Sinha SR, Kao JP, Bergles DE (2005) Ncm-D-aspartate: a novel caged D-aspartate suitable for activation of glutamate transporters and *N*-methyl-D-aspartate (NMDA) receptors in brain tissue. *Neuropharmacology* 49:831–842
11. Huang YH, Sinha SR, Fedoryak OD, Ellis-Davies GCR, Bergles DE (2005) Synthesis and characterization of 4-methoxy-7-nitroindolyl-D-aspartate, a caged compound for selective activation of glutamate transporters and *N*-methyl-D-aspartate receptors in brain tissue. *Biochemistry* 44:3316–3326
12. Ellis-Davies GCR (2007) Caged compounds: photorelease technology for control of cellular chemistry and physiology. *Nat Methods* 4:619–628
13. Fino E, Araya R, Peterka DS, Salierno M, Etchenique R, Yuste R (2009) RuBi-Glutamate: two-photon and visible-light photoactivation of neurons and dendritic spines. *Front Neural Circuits* 3:2
14. Gee KR, Wieboldt R, Hess GP (1994) Synthesis and photochemistry of a new photolabile derivative of GABA-neurotransmitter release and receptor activation in the microsecond time region. *J Am Chem Soc* 116:8366–8367
15. Cürten BC, Kullmann PHMK, Bier ME, Kandler KK, Schmidt BS (2005) Synthesis, photophysical, photochemical and biological properties of caged GABA, 4-[(2H-1-Benzopyran-2-one-7-amino-4-methoxy) carbonyl] amino] butanoic acid. *Photochem Photobiol* 81:641–648
16. Rial Verde EM, Zayat L, Etchenique R, Yuste R (2008) Photorelease of GABA with visible light using an inorganic caging group. *Front Neural Circuits* 2:2
17. Trigo FF, Papageorgiou G, Corrie JE, Ogden D (2009) Laser photolysis of DPNI-GABA, a tool for investigating the properties and distribution of GABA receptors and for silencing neurons in situ. *J Neurosci Methods* 181(2):159–169
18. Shembekar VR, Chen Y, Carpenter BK, Hess GP (2007) Coumarin-caged glycine that can be photolyzed within 3 microseconds by visible light. *Biochemistry* 46:5479–5484
19. Roitman MF, Stuber GD, Phillips PE, Wightman RM, Carelli RM (2004) Dopamine operates as a subsecond modulator of food seeking. *J Neurosci* 24:1265–1271
20. Sombers LA, Beyene M, Carelli RM, Wightman RM (2009) Synaptic overflow of dopamine in the nucleus accumbens arises from neuronal activity in the ventral tegmental area. *J Neurosci* 29:1735–1742

21. Breitinger HG, Wieboldt R, Ramesh D, Carpenter BK, Hess GP (2000) Synthesis and characterization of photolabile derivatives of serotonin for chemical kinetic investigations of the serotonin 5-HT₃ receptor. *Biochemistry* 39:5500–5508
22. Muralidharan S, Nerbonne JM (1995) Photolabile “caged” adrenergic receptor agonists and related model compounds. *J Photochem Photobiol B* 27:123–137
23. Lee TH, Gee KR, Ellinwood EH, Seidler FJ (1996) Combining “caged-dopamine” photolysis with fast-scan cyclic voltammetry to assess dopamine clearance and release autoinhibition in vitro. *J Neurosci Methods* 67:221–231
24. Kao JP (2006) Caged molecules: principles and practical considerations. *Curr Protoc Neurosci Chapter 6:Unit 6.20*
25. Kuner T, Li Y, Gee KR, Bonewald LF, Augustine GJ (2008) Photolysis of a caged peptide reveals rapid action of *N*-ethylmaleimide sensitive factor before neurotransmitter release. *Proc Natl Acad Sci USA* 105:347–352
26. Engels J, Schlaeager EJ (1977) Synthesis, structure, and reactivity of adenosine cyclic 3',5'-phosphate benzyl triesters. *J Med Chem* 20:907–911
27. Kaplan JH, Forbush B, Hoffman JF (1978) Rapid photolytic release of adenosine 5'-triphosphate from a protected analogue: utilization by the Na:K pump of human red blood cell ghosts. *Biochemistry* 17:1929–1935
28. Walker JW, Somlyo AV, Goldman YE, Somlyo AP, Trentham DR (1987) Kinetics of smooth and skeletal muscle activation by laser pulse photolysis of caged inositol 1,4,5-trisphosphate. *Nature* 327:249–252
29. Dantzig JA, Higuchi H, Goldman YE (1998) Studies of molecular motors using caged compounds. *Meth Enzymol* 291:307–348
30. Bamberg E, Clarke RJ, Fendler K (2001) Electrogenic properties of the Na⁺, K⁺-ATPase probed by presteady state and relaxation studies. *J Bioenerg Biomembr* 33:401–405
31. Adams SR, Tsien RY (1993) Controlling cell chemistry with caged compounds. *Annu Rev Physiol* 55:755–784
32. Kaplan JH, Ellis-Davies GCR (1988) Photolabile chelators for the rapid photorelease of divalent cations. *Proc Natl Acad Sci USA* 85:6571–6575
33. Ellis-Davies GCR, Kaplan JH (1994) Nitrophenyl-EGTA, a photolabile chelator that selectively binds Ca²⁺ with high affinity and releases it rapidly upon photolysis. *Proc Natl Acad Sci USA* 91:187–191
34. Makings LR, Tsien RY (1994) Caged nitric oxide. Stable organic molecules from which nitric oxide can be photoreleased. *J Biol Chem* 269:6282–6285
35. Ellis-Davies GCR (2008) Neurobiology with caged calcium. *Chem Rev* 108:1603–1613
36. Adams SR, Kao JPY, Tsien RY (1988) Biologically useful chelators that take up calcium (2+) upon illumination. *J Am Chem Soc* 111:7957–7968
37. Khodakhah K, Armstrong CM (1997) Inositol trisphosphate and ryanodine receptors share a common functional Ca²⁺ pool in cerebellar Purkinje neurons. *Biophys J* 73:3349–3357
38. Walker JW, Reid GP, Trentham DR (1989) Synthesis and properties of caged nucleotides. *Meth Enzymol* 172:288–301
39. Sarkisov DV, Wang SS-H (2008) Order-dependent coincidence detection in cerebellar Purkinje neurons at the inositol trisphosphate receptor. *J Neurosci* 28(1):133–142
40. Gee KR, Lee HC (1998) Characterization and application of photogeneration of calcium mobilizers cADP-ribose and nicotinic acid adenine dinucleotide phosphate from caged analogs. *Meth Enzymol* 291:403–415
41. Shirokova N, Niggli E (2008) Studies of RyR function in situ. *Methods* 46:183–193
42. Zhelyaskov VR, Godwin DW (1998) Photolytic generation of nitric oxide through a porous glass partitioning membrane. *Nitric Oxide* 2:454–459
43. Furuta T, Takeuchi H, Isozaki M, Takahashi Y, Kanehara M, Sugimoto M, Watanabe T, Noguchi K, Dore TM, Kurahashi T, Iwamura M, Tsien RY (2004) Bhc-cNMPs as either water-soluble or membrane-permeant photoreleasable cyclic nucleotides for both one- and two-photon excitation. *Chem-biochem* 5:1119–1128
44. Nerbonne JM (1996) Caged compounds: tools for illuminating neuronal responses and connections. *Curr Opin Neurobiol* 6:379–386
45. Lester HA, Nerbonne JM (1982) Physiological and pharmacological manipulations with light flashes. *Annu Rev Biophys Bioeng* 11:151–175
46. Gurney AM (1994) Flash photolysis of caged compounds. In: Ogden DA (ed) *Microelectrode techniques. The Plymouth workshop handbook. The company of Biologists* pp 389–406
47. Sarkisov DV, Wang SS-H (2007) Combining uncaging techniques with patch-clamp recording and optical physiology. In: Walz (ed) *Patch clamp analysis: advanced techniques*, vol 38, 2nd edn. Humana Press pp 149–168

48. Kramer RH, Chambers JJ, Trauner D (2005) Photochemical tools for remote control of ion channels in excitable cells. *Nat Chem Biol* 1:360–365
49. Szobota S, Gorostiza P, Del Bene F, Wyart C, Fortin DL, Kolstad KD, Tulyathan O, Volgraf M, Numano R, Aaron HL, Scott EK, Kramer RH, Flannery J, Baier H, Trauner D, Isacoff EY (2007) Remote control of neuronal activity with a light-gated glutamate receptor. *Neuron* 54:535–545
50. Gorostiza P, Volgraf M, Numano R, Szobota S, Trauner D, Isacoff EY (2007) Mechanisms of photoswitch conjugation and light activation of an ionotropic glutamate receptor. *Proc Natl Acad Sci USA* 104:10865–10870
51. Chambers JJ, Banghart MR, Trauner D, Kramer RH (2006) Light-induced depolarization of neurons using a modified shaker K⁺ channel and a molecular photoswitch. *J Neurophysiol* 96:2792–2796
52. Banghart M, Borges K, Isacoff E, Trauner D, Kramer RH (2004) Light-activated ion channels for remote control of neuronal firing. *Nat Neurosci* 7:1381–1386
53. Fortin DL, Banghart MR, Dunn TW, Borges K, Wagenaar DA, Gaudry Q, Karakossian MH, Otis TS, Kristan WB, Trauner D, Kramer RH (2008) Photochemical control of endogenous ion channels and cellular excitability. *Nat Methods* 5:331–338
54. Chambers JJ, Kramer RH (2008) Light-activated ion channels for remote control of neural activity. *Methods Cell Biol* 90:217–232
55. Knöpfel T (2008) Expanding the toolbox for remote control of neuronal circuits. *Nat Methods* 5:293–295
56. Nagel G, Szellas T, Huhn W, Kateriya S, Adeishvili N, Berthold P, Ollig D, Hegemann P, Bamberg E (2003) Channelrhodopsin-2, a directly light-gated cation-selective membrane channel. *Proc Natl Acad Sci USA* 100:13940–13945
57. Boyden ES, Zhang F, Bamberg E, Nagel G, Deisseroth K (2005) Millisecond-timescale, genetically targeted optical control of neural activity. *Nat Neurosci* 8:1263–1268
58. Zhang F, Wang LP, Boyden ES, Deisseroth K (2006) Channelrhodopsin-2 and optical control of excitable cells. *Nat Methods* 3:785–792
59. Ernst OP, Sánchez Murcia PA, Daldrop P, Tsunoda SP, Kateriya S, Hegemann P (2008) Photoactivation of channelrhodopsin. *J Biol Chem* 283:1637–1643
60. Nagel G, Brauner M, Liewald JF, Adeishvili N, Bamberg E, Gottschalk A (2005) Light activation of channelrhodopsin-2 in excitable cells of *Caenorhabditis elegans* triggers rapid behavioral responses. *Curr Biol* 15:2279–2284
61. Bamann C, Kirsch T, Nagel G, Bamberg E (2008) Spectral characteristics of the photocycle of channelrhodopsin-2 and its implication for channel function. *J Mol Biol* 375:686–694
62. Nikolic K, Grossman N, Grubb MS, Burrone J, Toumazou C, Degenaar P (2009) Photocycles of channelrhodopsin-2. *Photochem Photobiol* 85:400–411
63. Lin JY, Lin MZ, Steinbach P, Tsien RY (2009) Characterization of engineered channelrhodopsin variants with improved properties and kinetics. *Biophys J* 96:1803–1814
64. Berndt A, Yizhar O, Gunaydin LA, Hegemann P, Deisseroth K (2009) Bi-stable neural state switches. *Nat Neurosci* 12:229–234
65. Zhang F, Prigge M, Beyrière F, Tsunoda SP, Mattis J, Yizhar O, Hegemann P, Deisseroth K (2008) Red-shifted optogenetic excitation: a tool for fast neural control derived from *Volvox carteri*. *Nat Neurosci* 11:631–633
66. Zhang YP, Oertner TG (2006) Optical induction of synaptic plasticity using a light-sensitive channel. *Nat Methods* 4:139–141
67. Ishizuka T, Kakuda M, Araki R, Yawo H (2006) Kinetic evaluation of photosensitivity in genetically engineered neurons expressing green algae light-gated channels. *Neurosci Res* 54:85–94
68. Bormuth V, Howard J, Schaffer E (2007) LED illumination for video-enhanced DIC imaging of single microtubules. *J Microsc* 226:1–5
69. Benavides JM, Webb RH (2005) Optical characterization of ultrabright LEDs. *Appl Opt* 44:4000–4003
70. Lanyi JK (1990) Halorhodopsin, a light-driven electrogenic chloride-transport system. *Physiol Rev* 70(2):319–330
71. Han X, Boyden ES (2007) Multiple-color optical activation, silencing, and desynchronization of neural activity, with single-spike temporal resolution. *PLoS ONE* 2(3):e299
72. Zhang F, Wang LP, Brauner M, Liewald JF, Kay K, Watzke N, Wood PG, Bamberg E, Nagel G, Gottschalk A, Deisseroth K (2007) Multimodal fast optical interrogation of neural circuitry. *Nature* 446:633–639
73. Zhang F, Aravanis AM, Adamantidis A, de Lecea L, Deisseroth K (2007) Circuit-breakers: optical technologies for probing neural signals and systems. *Nat Rev Neurosci* 8:577–581

74. Gradinaru V, Thompson KR, Deisseroth K (2008) eNpHR: a *Natronomonas* halorhodopsin enhanced for optogenetic applications. *Brain Cell Biol* 36:129–139
75. Chow H, Qian XQ, Boyden ES (2009) High-performance halorhodopsin variants for improved genetically-targetable optical neural silencing. *Frontiers in systems neuroscience*. In: Conference abstract: computations and systems neuroscience
76. Gradinaru V, Mogri M, Thompson KR, Henderson JM, Deisseroth K (2009) Optical deconstruction of parkinsonian neural circuitry. *Science* 324:354–359
77. Sohal VS, Zhang F, Yizhar O, Deisseroth K (2009) Parvalbumin neurons and gamma rhythms enhance cortical circuit performance. *Nature* 459:698–702
78. Sjulson L, Miesenböck G (2008) Photocontrol of neural activity: biophysical mechanisms and performance in vivo. *Chem Rev* 108(5):1588–1602
79. Airan RD, Thompson KR, Fenno LE, Bernstein H, Deisseroth K (2009) Temporally precise in vivo control of intracellular signaling. *Nature* 458:1025–1029
80. Tsien RY (1989) Fluorescent probes of cell signaling. *Annu Rev Neurosci* 12:227–253
81. Stosiek C, Garaschuk O, Holthoff K, Konnerth A (2003) In vivo two-photon calcium imaging of neuronal networks. *Proc Natl Acad Sci USA* 100:7319–7324
82. Harvey CD, Svoboda K (2007) Locally dynamic synaptic learning rules in pyramidal neuron dendrites. *Nature* 450:1195–1202
83. Nikolenko V, Poskanzer KE, Yuste R (2007) Two-photon photostimulation and imaging of neural circuits. *Nat Methods* 4:943–950
84. Saito T (2006) In vivo electroporation in the embryonic mouse central nervous system. *Nat Protoc* 1:1552–1558
85. Tabata H, Nakajima K (2008) Labeling embryonic mouse central nervous system cells by *in utero* electroporation. *Dev Growth Differ* 50:507–511
86. Petreanu LP, Huber DH, Sobczyk AS, Svoboda KS (2007) Channelrhodopsin-2-assisted circuit mapping of long-range callosal projections. *Nat Neurosci* 10:663–668
87. Petreanu L, Mao T, Sternson SM, Svoboda K (2009) The subcellular organization of neocortical excitatory connections. *Nature* 457:1142–1145
88. Cetin A, Komai S, Eliava M, Seeburg PH, Osten P (2006) Stereotaxic gene delivery in the rodent brain. *Nat Protoc* 1:3166–3173
89. Adamantidis AR, Zhang F, Aravanis AM, Deisseroth K, de Lecea L (2007) Neural substrates of awakening probed with optogenetic control of hypocretin neurons. *Nature* 450:420–424
90. Dittgen T, Nimmerjahn A, Komai S, Licznarski P, Waters J, Margrie TW, Helmchen F, Denk W, Brecht M, Osten P (2004) Lentivirus-based genetic manipulations of cortical neurons and their optical and electrophysiological monitoring in vivo. *Proc Natl Acad Sci USA* 101:18206–18211
91. Bartlett JS, Wilcher R, Samulski RJ (2000) Infectious entry pathway of adeno-associated virus and adeno-associated virus vectors. *J Virol* 74:2777–2785
92. Wallace DJ, zum Alten Borgloh SM, Astori S, Yang Y, Bausen M, Kügler S, Palmer AE, Tsien RY, Sprengel R, Kerr JN, Denk W, Hasan MT (2008) Single-spike detection in vitro and in vivo with a genetic Ca(2+) sensor. *Nat Methods* 5:797–804
93. Song CK, Enquist LW, Bartness TJ (2005) New developments in tracing neural circuits with herpesviruses. *Virus Res* 111:235–249
94. Ekstrand MI, Enquist LW, Pomeranz LE (2008) The alpha-herpesviruses: molecular pathfinders in nervous system circuits. *Trends Mol Med* 14:134–140
95. Lima SQ, Hromádka T, Znamenskiy PZ, Zador AM (2009) Photostimulation-assisted identification of neuronal populations (PINP): a new method of tagging neuronal populations for identification during in vivo electrophysiological recording. *PLoS ONE* 4(7):e6099
96. Kuhlman SJ, Huang ZJ (2008) High-resolution labeling and functional manipulation of specific neuron types in mouse brain by Cre-activated viral gene expression. *PLoS ONE* 3:e2005
97. Atasoy D, Aponte Y, Su HH, Sternson SM (2008) A FLEX switch targets Channelrhodopsin-2 to multiple cell types for imaging and long-range circuit mapping. *J Neurosci* 28:7025–7030
98. Tsai HC, Zhang F, Adamantidis A, Stuber GD, Bonci A, de Lecea L, Deisseroth K (2009) Phasic firing in dopaminergic neurons is sufficient for behavioral conditioning. *Science* 324:1080–1084
99. Cardin JA, Carlén M, Meletis K, Knoblich U, Zhang F, Deisseroth K, Tsai LH, Moore CI (2009) Driving fast-spiking cells induces gamma rhythm and controls sensory responses. *Nature* 459:663–667

100. Schnütgen F, Doerflinger N, Calléja C, Wendling O, Chambon P, Ghyselinck NB (2003) A directional strategy for monitoring Cre-mediated recombination at the cellular level in the mouse. *Nat Biotechnol* 21:562–565
101. Davidson BL, Breakefield XO (2003) Viral vectors for gene delivery to the nervous system. *Nat Rev Neurosci* 4:353–364
102. Callaway EM (2008) Transneuronal circuit tracing with neurotropic viruses. *Curr Opin Neurobiol* 18:617–623
103. Hogan BH, Constantini FC, Lacey EL (1994) Production of transgenic mice. In: Hogan B, Beddington R, Constantini F, Lacey E (eds) *Manipulating the mouse embryo: a laboratory manual*. Cold Spring Harbor Laboratory Press, Cold Spring Harbor, NY, pp 217–252
104. Feng G, Mellor RH, Bernstein M, Keller-Peck C, Nguyen QT, Wallace M, Nerbonne JM, Lichtman JW, Sanes JR (2000) Imaging neuronal subsets in transgenic mice expressing multiple spectral variants of GFP. *Neuron* 28:41–51
105. Sprengel R, Hasan MT (2007) Tetracycline-controlled genetic switches. *Handb Exp Pharmacol* 178:49–72
106. Dymecki SM, Kim JC (2007) Molecular neuroanatomy's "three Gs": a primer. *Neuron* 54:17–34
107. Luo L, Callaway EM, Svoboda K (2008) Genetic dissection of neural circuits. *Neuron* 57:634–660
108. Arenkiel BR, Peca J, Davison IG, Feliciano C, Deisseroth K, Augustine GJ, Ehlers MD, Feng G (2007) In vivo light-induced activation of neural circuitry in transgenic mice expressing channelrhodopsin-2. *Neuron* 54:205–218
109. Liewald JF, Brauner M, Stephens GJ, Bouhours M, Schultheis C, Zhen M, Gottschalk A (2008) Optogenetic analysis of synaptic function. *Nat Methods* 5:895–902
110. Shoham S, O'Connor DH, Sarkisov DV, Wang SS-H (2005) Rapid neurotransmitter uncaging in spatially defined patterns. *Nat Methods* 2:837–843
111. Zipfel WR, Williams RM, Webb WW (2003) Nonlinear magic: multiphoton microscopy in the biosciences. *Nat Biotechnol* 21:1369–1377
112. Ellis-Davies GCR (2000) Basics of photoactivation. Yuste R, Lanni F, Konnerth A (eds) In: *Imaging neurons: a laboratory manual*. Cold Spring Harbor Laboratory Press, Cold Spring Harbor, NY, pp 24.1–24.8
113. Kandler K, Givens RS, Katz LC (2000) Photostimulation with caged glutamate. Yuste R, Lanni F, Konnerth A (eds) In: *Imaging neurons: a laboratory manual*. Cold Spring Harbor Laboratory Press, Cold Spring Harbor, NY, pp 27.1–27.9
114. Bernardinelli Y, Haeblerli C, Chatton JY (2005) Flash photolysis using a light emitting diode: an efficient, compact, and affordable solution. *Cell Calcium* 37:565–572
115. Venkataramani S, Davitt KM, Xu H, Zhang J, Song YK, Connors BW, Nurmikko AV (2007) Semiconductor ultra-violet light-emitting diodes for flash photolysis. *J Neurosci Methods* 160:5–9
116. Xu H, Zhang J, Davitt KM, Song Y, Nurmikko AV (2008) Application of blue-green and ultraviolet micro-LEDs to biological imaging and detection. *J Phys D Appl Phys* 41:94013
117. Pettit DL, Wang SS-H, Gee KR, Augustine GJ (1997) Chemical two-photon uncaging: a novel approach to mapping glutamate receptors. *Neuron* 19:465–471
118. Sarkisov DV, Gelber SE, Walker JW, Wang SS-H (2007) Synapse specificity of calcium release probed by chemical two-photon uncaging of inositol 1,4,5-trisphosphate. *J Biol Chem* 282:25517–25526
119. Wang SSH, Augustine GJ (1995) Confocal imaging and local photolysis of caged compounds: dual probes of synaptic function. *Neuron* 15:755–760
120. Matsuzaki M, Ellis-Davies GCR, Kasai H (2008) Three-dimensional mapping of unitary synaptic connections by two-photon macro photolysis of caged glutamate. *J Neurophysiol* 99:1535–1544
121. Göppert-Mayer M (1931) Über elementarakte mit zwei quantensprüngen. *Ann Phys* 9:273–294
122. Albota MA, Xu C, Webb WW (1998) Two-photon fluorescence excitation cross sections of biomolecular probes from 690 to 960 nm. *Appl Opt* 37:7352–7356
123. Gasparini S, Magee JC (2006) State-dependent dendritic computation in hippocampal CA1 pyramidal neurons. *J Neurosci* 26:2088–2100
124. Mohanty SK, Reinscheid RK, Liu X, Okamura N, Krasieva TB, Berns MW (2008) In-depth activation of ChR2 sensitized excitable cells with high spatial resolution using two-photon excitation with near-IR laser microbeam. *Biophys J* 95(8):3916–3926
125. Rickgauer JP, Tank DW (2009) Two-photon excitation of channelrhodopsin-2 at saturation. *Proc Natl Acad Sci USA* 106:15025–15030

126. Tang CM (2006) Photolysis of caged neurotransmitters: theory and procedures for light delivery. *Curr Protoc Neurosci* Chapter 6:Unit 6.21
127. Callaway EM, Katz LC (1993) Photostimulation using caged glutamate reveals functional circuitry in living brain slices. *Proc Natl Acad Sci USA* 90:7661–7665
128. Dalva MB, Katz LC (1994) Rearrangements of synaptic connections in visual cortex revealed by laser photostimulation. *Science* 265:255–258
129. Dantzker JL, Callaway EM (2000) Laminar sources of synaptic input to cortical inhibitory interneurons and pyramidal neurons. *Nat Neurosci* 3:701–707
130. Shepherd GM, Stepanyants A, Bureau I, Chklovskii D, Svoboda K (2005) Geometric and functional organization of cortical circuits. *Nat Neurosci* 8:782–790
131. Shepherd GM, Svoboda K (2005) Laminar and columnar organization of ascending excitatory projections to layer 2/3 pyramidal neurons in rat barrel cortex. *J Neurosci* 25:5670–5679
132. Major G, Polsky A, Denk W, Schiller J, Tank DW (2008) Spatiotemporally graded NMDA spike/plateau potentials in basal dendrites of neocortical pyramidal neurons. *J Neurophysiol* 99:2584–2601
133. Bliton AC, Lechleiter JD (1995) Optical considerations at ultraviolet wavelengths in confocal microscopy. In: Pawley JBY (ed) *Handbook of biological confocal microscopy*, 2nd edn. Plenum, New York, pp 431–444
134. Denk W, Delaney KR, Gelperin A, Kleinfeld D, Strowbridge BW, Tank DW, Yuste R (1994) Anatomical and functional imaging of neurons using 2-photon laser scanning microscopy. *J Neurosci Methods* 54:151–162
135. Tsai PS, Nishimura N, Yoder EJ, White A, Dolnick E, Kleinfeld D (2002) Principles, design and construction of a two photon scanning microscope for in vitro and in vivo studies. In: Frostig R (ed) *Methods for in vivo optical imaging*. CRC Press pp 113–171
136. Gasparini S, Losonczy A, Chen X, Johnston D, Magee JC (2007) Associative pairing enhances action potential back-propagation in radial oblique branches of CA1 pyramidal neurons. *J Physiol* 580:787–800
137. Lörincz A, Rózsa B, Katona G, Vizi ES, Tamás G (2007) Differential distribution of NCX1 contributes to spine-dendrite compartmentalization in CA1 pyramidal cells. *Proc Natl Acad Sci USA* 104:1033–1038
138. Lillis KP, Eng A, White JA, Mertz J (2008) Two-photon imaging of spatially extended neuronal network dynamics with high temporal resolution. *J Neurosci Methods* 172:178–184
139. Göbel W, Kampa BM, Helmchen F (2006) Imaging cellular network dynamics in three dimensions using fast 3D laser scanning. *Nat Methods* 4:73–79
140. Bullen A, Patel SS, Saggau P (1997) High-speed, random-access fluorescence microscopy I. High-resolution optical recording with voltage-sensitive dyes and ion indicators. *Biophys J* 73(1):477–491
141. Kremer Y, Léger JF, Lapole R, Honnorat N, Candela Y, Dieudonné S, Bourdieu L (2008) A spatio-temporally compensated acousto-optic scanner for two-photon microscopy providing large field of view. *Opt Express* 16:10066–10076
142. Reddy G, Kelleher K, Fink R, Saggau P (2008) Three-dimensional random access multiphoton microscopy for functional imaging of neuronal activity. *Nat Neurosci* 11:713–720
143. Oheim M, Beaurepaire E, Chaigneau E, Mertz J, Charpak S (2001) Two-photon microscopy in brain tissue: parameters influencing the imaging depth. *J Neurosci Methods* 111:29–37
144. Gerchberg RW, Saxton WO (1972) A practical algorithm for the determination of the phase from image and diffraction plane pictures. *Optik* 35:237–246
145. Lutz C, Otis TS, Desars V, Charpak S, Digregorio DA, Emiliani V (2008) Holographic photolysis of caged neurotransmitters. *Nat Methods* 5(9):821–827
146. Nikolenko V, Watson BO, Araya R, Woodruff A, Peterka DS, Yuste R (2008) SLM microscopy: scanless two-photon imaging and photostimulation with spatial light modulators. *Front Neural Circuits* 2:5
147. Pologruto TA, Sabatini BL, Svoboda K (2003) ScanImage: flexible software for operating laser-scanning microscopes. *Biomed Eng Online* 2:13
148. Hoogland TM, Kuhn B, Göbel W, Huang W, Nakai J, Helmchen F, Flint J, Wang SS (2009) Radially expanding transglial calcium waves in the intact cerebellum. *Proc Natl Acad Sci USA* 106:3496–3501
149. Iyer V, Losavio BE, Saggau P (2003) Compensation of spatial and temporal dispersion for acousto-optic multiphoton laser-scanning microscopy. *J Biomed Opt* 8:460

150. Salomé R, Kremer Y, Dieudonné S, Léger JF, Krichevsky O, Wyart C, Chatenay D, Bourdieu L (2006) Ultrafast random-access scanning in two-photon microscopy using acousto-optic deflectors. *J Neurosci Methods* 154:161–174
151. Zeng S, Lv X, Zhan C, Chen WR, Xiong W, Jacques SL, Luo Q (2006) Simultaneous compensation for spatial and temporal dispersion of acousto-optical deflectors for two-dimensional scanning with a single prism. *Opt Lett* 31:1091–1093
152. Friedman N, Kaplan A, Davidson N (2000) Acousto-optic scanning system with very fast nonlinear scans. *Opt Lett* 25:1762–1764
153. Reddy GD, Saggau P (2005) Fast three-dimensional laser scanning scheme using acousto-optic deflectors. *J Biomed Opt* 10(6):064038
154. Chang IC, Assoc A, Santa Clara CA (1994) Acousto-optic modulator with wide bandwidth and large angular aperture. *Electron Lett* 30:1190–1191
155. Vučinić D, Sejnowski TJ (2007) A compact multiphoton 3D imaging system for recording fast neuronal activity. *PLoS ONE* 2:8
156. Oron D, Silberberg Y (2005) Spatiotemporal coherent control using shaped, temporally focused pulses. *Opt Express* 13:9903–9908
157. Papagiakoumou E, de Sars V, Oron D, Emiliani V (2008) Patterned two-photon illumination by spatiotemporal shaping of ultra-short pulses. *Opt Express* 16:22039–22047
158. Oku H, Hashimoto K, Ishikawa M (2004) Variable-focus lens with 1-kHz bandwidth. *Opt Express* 12:2138–2149
159. Zhu L, Sun PC, Fainman Y (1999) Aberration-free dynamic focusing with a multichannel micromachined membrane deformable mirror. *Appl Opt* 38:5350–5354
160. Amir W, Carriles R, Hoover EE, Planchon TA, Durfee CG, Squier JA (2007) Simultaneous imaging of multiple focal planes using a two-photon scanning microscope. *Opt Lett* 32:1731–1733
161. Rózsa B, Katona G, Vizi ES, Várallyay Z, Ságghy A, Valenta L, Maák P, Fekete J, Bánysz A, Szipocs R (2007) Random access three-dimensional two-photon microscopy. *Appl Opt* 46:1860–1865
162. Keller M, Kao JPY, Egger M, Niggli E, (2007) Calcium waves driven by “sensitization” wavefronts. *Cardiovasc Res* 74:39–45
163. Kirleby PA, Naga Srinivas NKM, Silver RA (2010) A compact acousto-optic lens for 2D and 3D femtosecond based 2-photon microscopy. *Opt Express* 18:13721–13745



<http://www.springer.com/978-1-61779-030-0>

Photosensitive Molecules for Controlling Biological
Function

Chambers, J.J.; Kramer, R.H. (Eds.)

2011, XIV, 297 p., Hardcover

ISBN: 978-1-61779-030-0

A product of Humana Press